

This is an Open Access document downloaded from ORCA, Cardiff University's institutional repository:<https://orca.cardiff.ac.uk/id/eprint/130174/>

This is the author's version of a work that was submitted to / accepted for publication.

Citation for final published version:

Zagorščak, Renato , Sadasivam, Sivachidambaram , Thomas, Hywel Rhys , Stańczyk, Krzysztof and Kapusta, Krzysztof 2020. Experimental study of underground coal gasification (UCG) of a high-rank coal using atmospheric and high-pressure conditions in an ex-situ reactor. *Fuel* 270 , 117490. 10.1016/j.fuel.2020.117490

Publishers page: <http://doi.org/10.1016/j.fuel.2020.117490>

Please note:

Changes made as a result of publishing processes such as copy-editing, formatting and page numbers may not be reflected in this version. For the definitive version of this publication, please refer to the published source. You are advised to consult the publisher's version if you wish to cite this paper.

This version is being made available in accordance with publisher policies. See <http://orca.cf.ac.uk/policies.html> for usage policies. Copyright and moral rights for publications made available in ORCA are retained by the copyright holders.



1 Experimental study of underground coal gasification (UCG) of a high-  
2 rank coal using atmospheric and high-pressure conditions in an ex-  
3 situ reactor

4 Renato Zagorščak <sup>a,\*</sup>, Sivachidambaram Sadasivam <sup>a</sup>, Hywel Rhys Thomas <sup>a</sup>, Krzysztof

5 Stańczyk <sup>b</sup>, Krzysztof Kapusta <sup>b</sup>

6 <sup>a</sup> *Geoenvironmental Research Centre (GRC), School of Engineering, Cardiff University, The*  
7 *Queen's Buildings, The Parade, Cardiff, CF24 3AA, United Kingdom*

8 <sup>b</sup> *Główny Instytut Górnictwa (Central Mining Institute), Plac Gwarków 1, 40-166 Katowice,*  
9 *Poland*

10 **Abstract:**

11 This paper presents the results of an extensive experimental analysis of underground coal gasification  
12 (UCG) using large bulk samples in an ex-situ reactor under atmospheric and high-pressure (30 bar)  
13 conditions. The high-rank coal obtained from the South Wales (UK) coalfield is employed for that  
14 purpose. The aim of this investigation is to define the gas production rates, gas composition, gas  
15 calorific value, process energy efficiency and temperature changes within the UCG reactor during the  
16 gasification process based on the pre-defined reactants and flow rates. Two UCG trials, each lasting  
17 105 hours, consisted of six stages where the influences of oxygen, water, air and oxygen enriched air  
18 (OEA) under different flow conditions on the gasification process were investigated. Based on the  
19 results of two multi-day experiments, it is demonstrated that the gasification under high pressure  
20 conditions produces syngas with higher average calorific value (8.49 MJ/Nm<sup>3</sup>) in comparison to syngas  
21 produced at atmospheric pressure conditions (6.92 MJ/Nm<sup>3</sup>). Hence, the overall energy efficiency of  
22 the high-pressure experiment is higher compared to the atmospheric pressure test, i.e. 57.67%  
23 compared to 51.72%. This is related to the fact that the high-pressure gasification produces more  
24 methane (11.97 vol.%) than the atmospheric pressure gasification (2.30 vol.%). Under elevated  
25 pressure, the temperatures recorded in the roof strata are about 100°C higher compared to the UCG  
26 process under atmospheric pressure conditions. This work provides new insights into the gasification  
27 of carbon-rich coals subject to different gasification regimes and pressures.

28 **Keywords:**

29 Underground coal gasification; coal; high pressure; syngas; anthracite; in-situ laboratory tests

30 **\* Corresponding author:**

31 Renato Zagorščak  
32 ZagorscakR@cardiff.ac.uk  
33 +44 (0) 29208 76264  
34 Geoenvironmental Research Centre (GRC)  
35 School of Engineering, Cardiff University  
36 The Queen's Buildings  
37 The Parade  
38 CF24 3AA  
39 Cardiff  
40 United Kingdom

## 41 1. Introduction

42 Climate change represents a great threat to human society and the planet and there is an urgent need  
43 to limit the global warming to 1.5°C above pre-industrial levels by adopting greenhouse gas emissions  
44 pathways and low-carbon technologies to achieve a cost-effective transition [1]. On a global scale, it  
45 will be necessary to remove around 810 Gt of CO<sub>2</sub> by 2100 to achieve such target [2]. However, the  
46 rising incomes and an extra 1.7 billion people, predominantly in the urban areas of the developing  
47 economies, is expected to push up the global energy demand by more than a quarter to 2040 [3]. As  
48 the fossil fuels will remain a major part of the global energy mix accounting for around 40% of primary  
49 energy use in 2050 [4], the environmental footprint of the existing and emerging technologies must  
50 therefore be reduced and kept to a minimum.

51 One of the technologies that offer a prospect towards the transition in the low-carbon future is the  
52 Underground Coal Gasification (UCG) through which deep coal deposits can be utilised for the in-situ  
53 production of a synthetic gas predominantly consisting of hydrogen, methane, carbon monoxide and  
54 carbon dioxide [5, 6]. As the coal reserves significantly exceed those of oil and gas, and less than one  
55 sixth of the world's coal is economically accessible, UCG offers a possibility to utilise such reserves in  
56 a more environmentally safer way than the conventional mining techniques by eliminating mine safety  
57 issues, surface damage and solid waste at the surface [7]. Furthermore, potential UCG sites are often  
58 in the vicinity of geological formations suitable for CO<sub>2</sub> sequestration or enhanced oil recovery in which  
59 the CO<sub>2</sub> generated by UCG could be stored [7, 8].

60 UCG has a history of development around the world [8], with the majority of field trials being  
61 conducted in the United States [9-11], European Union [12-14], China [15], Australia [16] and the  
62 former Soviet Union [17]. Most trials have demonstrated that the UCG can be successfully conducted  
63 and that under specific geological and thermodynamic conditions, environmental impact can be  
64 minimised. However, despite its potential and over a century of development, UCG has still not been  
65 commercialised.

66 The UCG provides a potential mean for the recovery of energy from deep coal deposits that are  
67 uneconomic to mine. Hence, conducting experimental investigations on coals of different rank under  
68 elevated pressures and using a range of gasification reagents under different flow regimes is required.  
69 This would provide further understanding of the UCG technology and its impact on the environment  
70 under relevant conditions. Up to date, a large amount of experimental research work has been  
71 conducted on bituminous, sub-bituminous and lignite coals predominantly under atmospheric  
72 pressure conditions [18-25]. Only a small number of researchers performed gasification experiments  
73 under elevated pressures, however, on low rank coals [26, 27] or in small-scale [28, 29]. Hence, as the  
74 composition of the product gas and the efficiency of the UCG process depend on the thermodynamic  
75 conditions of the process, the coal composition as well as the gasifying agent used, further information  
76 of both atmospheric and high pressure gasification processes in large-scale obtained during injection  
77 of different gasification reagents on carbon-rich coals is required.

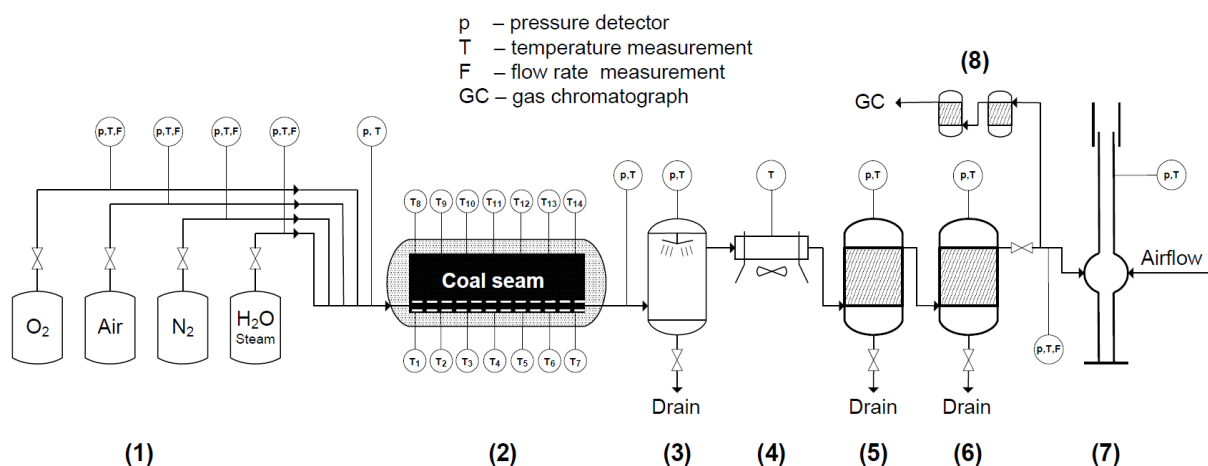
78 This study deals with the large-scale ex-situ gasification of high-rank coal obtained from the South  
79 Wales coalfield, UK both at atmospheric and high-pressure (30 bar) conditions using a range of  
80 gasification reagents under different flow regimes. Prior to the gasification experiments, the coal was  
81 characterised using Proximate and Ultimate analyses, sulphur form analysis and petrographic  
82 composition. Two multi-days trials, each lasting 105 hours, were carried out using artificial coal seams  
83 each with a mass of 650 kg, as described below. The experiments involved testing the influence of  
84 gasifying medium (oxygen, water, air and oxygen enriched air – OEA) under different flow and  
85 pressure conditions on the syngas composition and overall process efficiency. Furthermore,  
86 temperature changes within the reactor were continuously monitored throughout each experiment.

87 This work provides new insights into the gasification of high-rank coal as well as the coal from the  
88 South Wales coalfield demonstrating its applicability for UCG technology.

## 89 2. Experimental setup and methodology

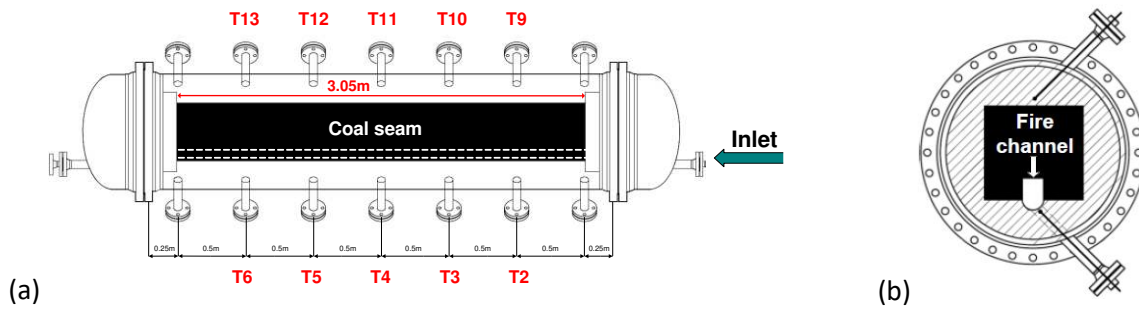
### 90 2.1. Ex-situ high-pressure UCG facility

91 The experimental simulations of UCG process involved the use of large-scale laboratory facilities of  
 92 Główny Instytut Górnictwa's (GIG) Clean Coal Technology Centre located at Experimental Mine  
 93 "Barbara" in Mikołów, Poland [26, 27]. The gasification chamber used as a part of the ex-situ surface  
 94 installation enables simulations of UCG in an artificial coal seam (max. seam length 3.5 m, cross section  
 95  $0.41 \times 0.41$  m) where gasification media like oxygen, air, steam and hydrogen can be used (Fig. 1).  
 96 Maximum gasification pressure and temperature that can be achieved and controlled within the  
 97 chamber are 50 bar and 1600 °C, respectively. Concentrations of the main gaseous components were  
 98 analysed using gas chromatography technique where the product gas was sampled every 30 minutes.  
 99 Concentrations of CH<sub>4</sub>, H<sub>2</sub>, CO, CO<sub>2</sub>, C<sub>2</sub>H<sub>6</sub>, N<sub>2</sub> and H<sub>2</sub>S within the gas mixture were determined.  
 100 Distribution of temperature during the gasification process was controlled by ten high-temperature  
 101 thermocouples, i.e. five placed in the gasification channel and five in the roof strata (Fig. 2a). The first  
 102 thermocouples (T2 and T9) were placed 0.5 m away from the face of the coal seam (inlet of the  
 103 reactor). Remaining thermocouples (T3-T6 and T10-T13) were then spaced 0.5 m apart. In order to  
 104 protect them from direct contact with oxidizers, the thermocouples were placed in the insulating  
 105 layer, approximately 2 cm from the bottom and roof of the artificial coal seam (Fig. 2b). Further details  
 106 on the experimental facility can be found elsewhere [26, 27].



107

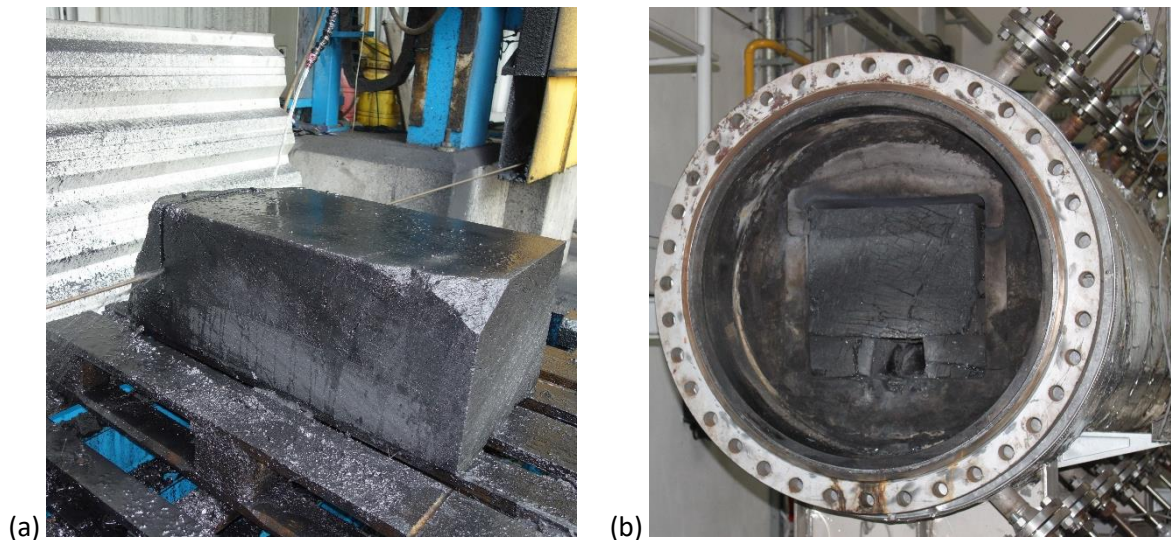
108 **Fig. 1.** Scheme of the ex-situ high-pressure UCG installation: (1) compressed reagents, (2) pressure  
 109 reactor, (3) wet scrubber for gas cleaning, (4) air cooler, (5, 6) gas separators, (7) thermal combustor,  
 110 (8) gas treatment module prior to GC analysis.



111 **Fig. 2.** (a) Pressure reactor side cross-section, (b) pressure reactor longitudinal cross-section.

112 2.2. Sample preparation and characterisation

113 Six large coal blocks were collected from an open cast coal mine in the South Wales coalfield, close to  
 114 Merthyr Tydfil, UK. The coal blocks belong to the Gellideg coal seam and were obtained from 135 m  
 115 below the original ground level, i.e. 262 m above ordnance datum. Upon extraction, the coal blocks  
 116 were wrapped in cling film to minimize the oxidation of the coal surfaces and preserve chemical and  
 117 physical properties, and then put in wooden crates to be transported to the laboratory at GIG for  
 118 further analysis and preparation. Upon arrival to GIG, raw coal samples were processed using a  
 119 diamond rope saw to create a continuous artificial coal seam of a total length of 3.05 m, a width of  
 120 0.41 m and a thickness of 0.41 m. The artificial coal seam in each experiment was prepared from 5  
 121 block samples of provided coal which were loaded in the reactor using a chain block hoist and ratchet  
 122 straps, and then pushed together using a forklift ensuring minimum gap between the blocks (Fig. 3).  
 123 The total mass of each continuous coal seam used for the experiments was approximately 650 kg  
 124 (Table 1).



125 **Fig. 3.** Preparation of the artificial coal seams for UCG tests: (a) Coal blocks being processed, (b) The  
 126 reaction chamber loaded with coal.

127 Table 1. Dimensions and weights of coal blocks used for UCG tests.

Coal block	Width (m)	Height (m)	Length (m)	Weight (kg)
Atmospheric pressure experiment				
1	0.41	0.41	0.73	155
2	0.41	0.41	0.77	163
3	0.41	0.41	0.64	135
4	0.41	0.41	0.26	55
5	0.41	0.41	0.66	140
High-pressure (30 bar) experiment				
1	0.41	0.41	0.35	75
2	0.41	0.41	0.88	187
3	0.41	0.41	0.84	179
4	0.41	0.41	0.62	132
5	0.41	0.41	0.36	77

128 Small pieces of coal were collected from large blocks to be used for coal characterisation which  
 129 included Proximate and Ultimate analyses, sulphur form analysis and petrographic composition. All  
 130 analyses were performed by Department of Solid Fuels Quality Assessment of GIG and the results are  
 131 presented in Table 2. Based on the results obtained and the comparison with the ASTM [30]  
 132 classification of coal rank, this coal can be classified as semi-anthracite.

133 Table 2. Characteristics of coal used for gasification experiments.

Parameter	Value
<b>As received</b>	
Total moisture (%)	1.15 ± 0.40
Ash (%)	4.61 ± 0.3
Volatiles (%)	9.92 ± 0.12

Total sulphur (%)	1.55 ± 0.04
Calorific value (kJ/kg)	33,416 ± 220
<b>Analytical</b>	
Moisture (%)	0.84 ± 0.30
Ash (%)	4.62 ± 0.3
Volatiles (%)	9.95 ± 0.13
Heat of combustion (kJ/kg)	34,414 ± 228
Calorific value (kJ/kg)	33,527 ± 221
Total sulphur (%)	1.55 ± 0.04
Carbon (%)	87.31 ± 0.66
Hydrogen (%)	3.97 ± 0.28
Nitrogen (%)	1.29 ± 0.12
Oxygen (%)	0.50 ± 0.05
Specific gravity (g/cm <sup>3</sup> )	1.35 ± 0.028
<b>Maceral group</b>	
Vitrinite (%)	72 ± 6
Liptinite (%)	0 ± 1
Inertinite (%)	28 ± 3
Vitrinite Reflectance (%)	1.67 ± 0.03
<b>Sulphur form</b>	
Total sulphur (%)	1.55 ± 0.04
Pyritic sulphur (%)	0.75 ± 0.07
Sulphate sulphur (%)	0.05 ± 0.02
Ash sulphur (%)	0.08 ± 0.01
Combustible sulphur (%)	1.47 ± 0.07

---

134        2.3.        Experimental procedure

135        Two multiday underground coal gasification trials, each lasting 105 hours, were conducted, i.e. one at  
136        atmospheric pressure and one at high pressure (30 bar) conditions. The particular stages of the UCG  
137        tests are shown in Table 3. Each experiment was divided in six stages, based on the type of gasification  
138        reagent and flow rates used. Different stages were considered to assess the impact of various  
139        gasification agents on the gas composition and calorific value, as changes in the gasification reagent  
140        can be helpful when the gas calorific value decreases as the cavity is growing. Such results can provide  
141        initial assessment of the value of the product gas against a particular gasification reagent as different  
142        reactants and product gases are associated with specific financial costs/benefits during in-situ  
143        gasification. The coal seams were ignited using a pyrotechnic charge located inside the gasification  
144        channel at the bottom of the coal seam at a distance of approximately 1 m from the face of the coal  
145        seam. The gasification process was started by putting oxygen (99.5% purity) into the ignited coal seam.  
146        Upon finishing the experiments, nitrogen was used for extinguishing and cooling down purpose.

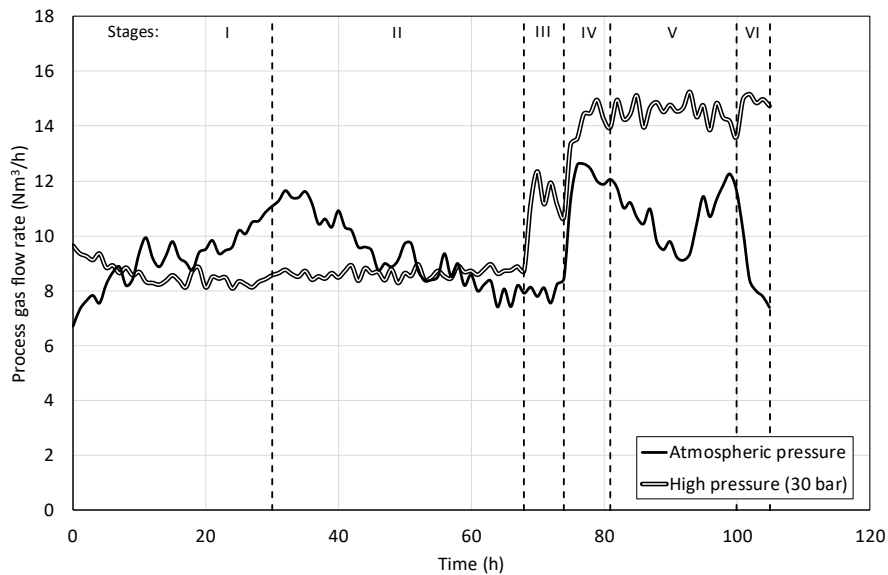
147 Table 3. Stages of the underground coal gasification experiments.

Stage	Gasification reagent	Flow rates (Nm <sup>3</sup> /h)		Duration (h)
		Atmospheric pressure experiment	High-pressure (30 bar) experiment	
I	Oxygen	5	5	30
II	Oxygen + water	5 (O <sub>2</sub> ) + 2.5 (H <sub>2</sub> O)	5 (O <sub>2</sub> ) + 2.5 (H <sub>2</sub> O)	38
III	Air	6	8	6
IV	Air	10	12	7
V	OEA 50%	5 (air) + 3 (O <sub>2</sub> )	7.5 (air) + 4.5 (O <sub>2</sub> )	19
VI	OEA 50% + water	5 (air) + 3 (O <sub>2</sub> ) + 2.5 (H <sub>2</sub> O)	7.5 (air) + 4.5 (O <sub>2</sub> ) + 2.5 (H <sub>2</sub> O)	5
Total:				105

148 **3. Results and discussion**

149 **3.1. Gas production rates**

150 The gas production rates as a function of time for the experiments conducted at atmospheric and high  
 151 pressure (30 bar) are presented in Fig. 4. Overall, the high-pressure experiment provided more stable  
 152 gas production than the atmospheric one. In particular, during the first stage of gasification using  
 153 oxygen, the production rate in the atmospheric pressure test was continuously increasing from 7  
 154 Nm<sup>3</sup>/h to 10.9 Nm<sup>3</sup>/h, while in the high pressure one it was constant at around 8.3 Nm<sup>3</sup>/h. The  
 155 production rate obtained at atmospheric pressure conditions was then continuously decreasing to 8  
 156 Nm<sup>3</sup>/h, while the change at high-pressure conditions was negligible. Introducing air as a gasification  
 157 reagent in the third stage did not induce any significant changes in the flow rates obtained at  
 158 atmospheric pressure conditions, however the flow rates increased up to a maximum of 12.4 Nm<sup>3</sup>/h  
 159 at high-pressure experiment. During the fourth stage, the flow rates obtained in the high-pressure  
 160 experiment increased to 15 Nm<sup>3</sup>/h and remained nearly constant throughout the fifth and sixth stages.  
 161 For the experiment conducted at atmospheric pressure conditions, the flow rate increased in the  
 162 fourth stage to 12.6 Nm<sup>3</sup>/h, followed by a decline in stage five until reaching 9.1 Nm<sup>3</sup>/h and then  
 163 rebounding to 12.3 Nm<sup>3</sup>/h towards the end of the stage. In the sixth stage, a rapid decrease in the  
 164 flow rates occurred reaching 7.4 Nm<sup>3</sup>/h by the end of the experiment. The reason for rapid decline in  
 165 Stages 5 and 6 is unknown but may be related to the spalling of the gasified material into the  
 166 gasification channel and reducing the gas flow within the reactor.

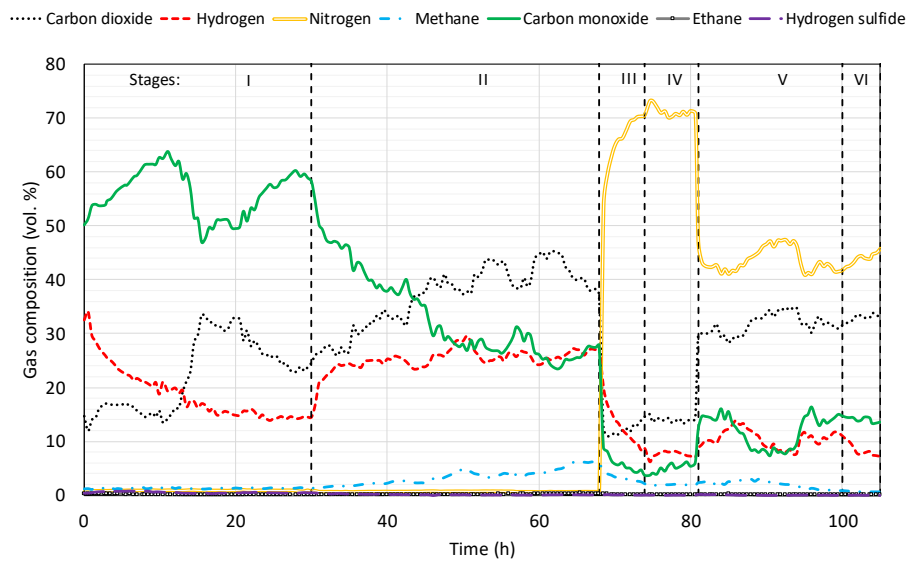


167  
 168 **Fig. 4.** Gas production over the course of the atmospheric and high-pressure (30 bar) UCG  
 169 experiments.

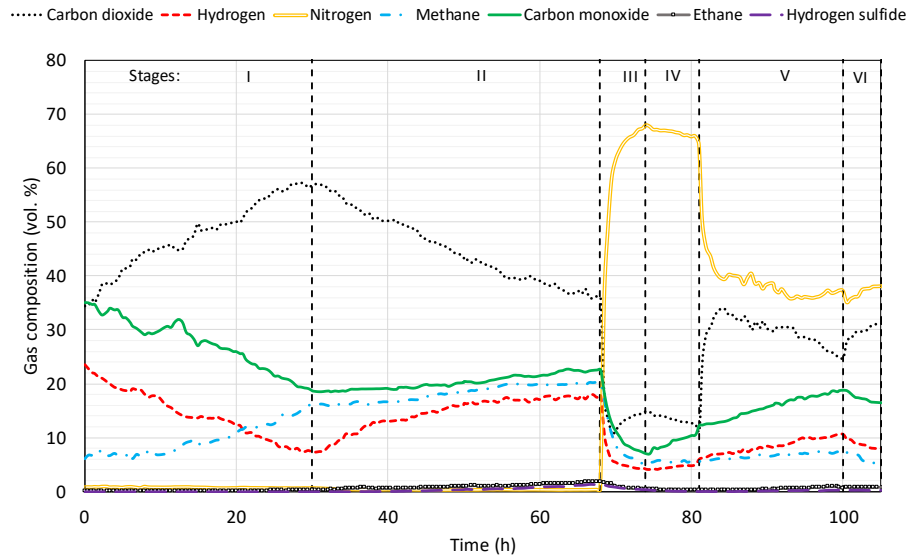
170 3.2. Gas composition and gas calorific value

171 Changes in the gas composition obtained over the course of the atmospheric and high-pressure  
 172 experiments are presented in Fig. 5a and Fig. 5b, respectively. During the 1<sup>st</sup> stage of both  
 173 experiments, CH<sub>4</sub> concentration was steadily increasing, opposite to H<sub>2</sub> concentration. However, the  
 174 30 bar experiment showed higher rate of CH<sub>4</sub> increase than the atmospheric one. Adding steam to  
 175 oxygen in the 2<sup>nd</sup> stage initiated an increase in CH<sub>4</sub> and H<sub>2</sub> concentrations for both atmospheric and  
 176 30 bar experiments, yielding maximum concentrations of 6.2% and 20.3% of CH<sub>4</sub> and 27.4% and 17.9%  
 177 of H<sub>2</sub> by the end of the stage, respectively. Presence of steam benefits H<sub>2</sub> generation through steam  
 178 gasification and water gas shift reactions which then participates in the hydrogasification and Sabatier  
 179 reactions favoured at high pressure increasing the production of CH<sub>4</sub>. During the 3<sup>rd</sup>-6<sup>th</sup> stages of the  
 180 experiment conducted at atmospheric pressure when air was introduced in the system, CH<sub>4</sub>  
 181 concentration experienced a steady drop reaching 0.6% by the end of the experiment. For the high-  
 182 pressure experiment, CH<sub>4</sub> generation was more stable as it decreased to 5.12% during the air  
 183 gasification stage but then remained nearly constant throughout 4<sup>th</sup>-6<sup>th</sup> stages. H<sub>2</sub> generation rapidly  
 184 decreased at the beginning of the 3<sup>rd</sup> stage and then slowly increased towards the end of both  
 185 experiments as more oxygen and steam were added throughout stages 4-6. Generation of CO followed

186 the same pattern as H<sub>2</sub> production in stages 3-6, however the first two stages in both experiments  
 187 were marked with high CO generation accompanied by high CO<sub>2</sub> concentrations due to strong  
 188 oxidation reactions initiated by high concentration of O<sub>2</sub> in the reactor. Concentrations of 58.9% and  
 189 35.1% of CO, and 45.4% and 57.3% of CO<sub>2</sub> were observed in atmospheric and 30 bar experiments,  
 190 respectively. Injection of air in stages 3-4 decreased the CO<sub>2</sub> generation but increased the N<sub>2</sub> portion  
 191 in the gas mixture instead, yielding N<sub>2</sub> concentrations in the region of 65-73% in the atmospheric  
 192 pressure test and 63-68% in the high-pressure test. Small amounts of C<sub>2</sub>H<sub>6</sub> and H<sub>2</sub>S were measured in  
 193 both experiments, with the maximum recorded concentrations of 0.37% and 0.84%, and 1.89% and  
 194 1.35% at the end of the 2<sup>nd</sup> stage of the atmospheric and high-pressure experiments, respectively.



(a)



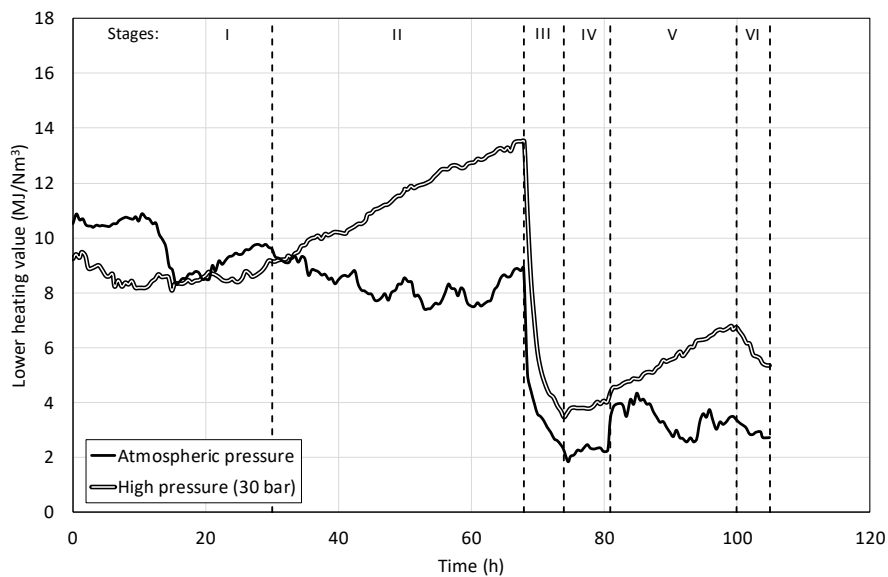
(b)

195 **Fig. 5.** Gas composition over the course of the UCG experiments: (a) atmospheric gasification, (b) high-  
 196 pressure (30 bar) gasification.

197 Changes in the gas calorific values over the course of both experiments are presented in Fig. 6. As  
 198 shown for the atmospheric pressure experiment, the maximum gas calorific value of 10.9 MJ/Nm<sup>3</sup> was  
 199 obtained during the oxygen gasification (the 1<sup>st</sup> stage). In the subsequent stages, the calorific value of  
 200 the produced gas has shown a decrease reaching a minimum of 1.8 MJ/Nm<sup>3</sup> during the air gasification  
 201 (the 3<sup>rd</sup> and 4<sup>th</sup> stages). During the high-pressure experiment, the gas calorific value was nearly  
 202 constant at around 8.6 MJ/Nm<sup>3</sup> in the 1<sup>st</sup> stage and then steadily increasing throughout the 2<sup>nd</sup> stage  
 203 (oxygen and water gasification) reaching a maximum value of 13.52 MJ/Nm<sup>3</sup>. During the air  
 204 gasification, the gas calorific value experienced a sudden drop to a minimum of 3.5 MJ/Nm<sup>3</sup> followed  
 205 by a recovery with a maximum value of 6.8 MJ/Nm<sup>3</sup> during the OEA gasification.

206 The changes of gas composition came as a result of several influencing factors such as thermodynamic  
 207 conditions as well as the composition and temperature of the gasifying agent used. During the oxygen  
 208 injection, the gasification process is primarily governed by highly exothermic reactions which increase  
 209 the temperature of the system and produce high concentrations of CO and CO<sub>2</sub>. Relatively high  
 210 concentration of H<sub>2</sub> in the 1<sup>st</sup> stage can be partially explained through chemical reactions involving an  
 211 inherent coal moisture. CH<sub>4</sub> production comes primarily as a result of the methanation reaction.  
 212 However, a relatively high concentration of CH<sub>4</sub> was observed in the high-pressure test compared to

213 the atmospheric pressure test confirming that CH<sub>4</sub> generation is favoured under high pressure  
 214 conditions. As the water was introduced into the system in the 2<sup>nd</sup> stage, both the H<sub>2</sub> and CH<sub>4</sub> contents  
 215 increased, but CO content decreased as a result of the steam gasification and water-gas shift reaction.  
 216 Consequently, this only improved the gas calorific value in the high-pressure experiment which  
 217 experienced a more significant increase in the CH<sub>4</sub> content and less reduction in the CO content  
 218 compared to the atmospheric pressure test. During the air gasification, the gas calorific value reduced  
 219 significantly as a result of the decrease in the amount of combustible components in the product gas.  
 220 During the air injection, nitrogen is the main product gas as it does not participate in the main  
 221 gasification reactions. During the OEA and OEA with water injection, the calorific value of the product  
 222 gas improves as a result of the increased oxygen content in the reactant gas which increases the  
 223 temperature in the coal seam and positively affects the gas quality.



224  
 225 **Fig. 6.** Changes in gas calorific values over the course of the atmospheric and high-pressure (30 bar)  
 226 UCG experiments.

227 Table 4 presents the average gas compositions and calorific values obtained during both atmospheric  
 228 and high-pressure experiments. If the calorific values are compared between the particular stages of  
 229 each experiment, all stages of the 30 bar experiment except the 1<sup>st</sup> one result in a higher average  
 230 calorific value compared to the atmospheric pressure experiment. This exception is related to the  
 231 rapid development of oxidation zone in the atmospheric gasification which increased the temperature

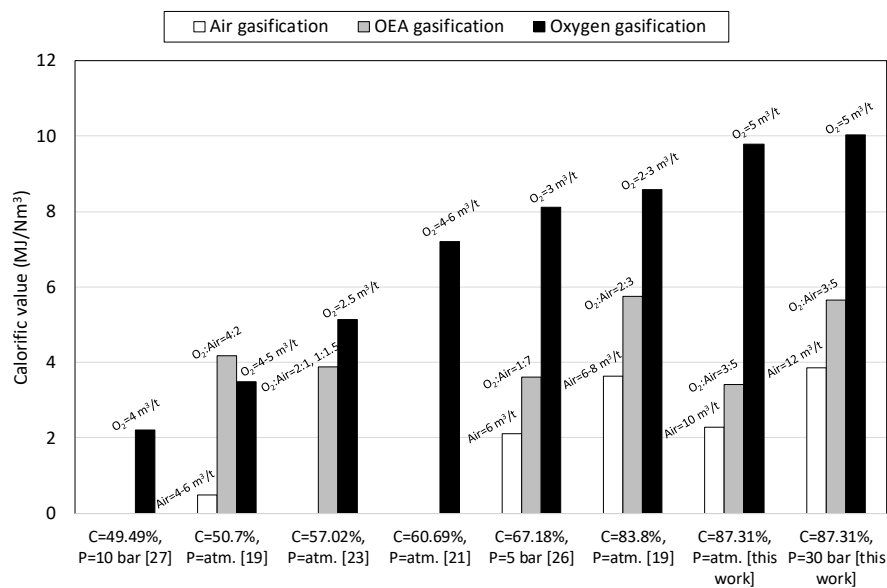
232 of the system and enhanced the production of CO and H<sub>2</sub>. Overall, the atmospheric test produced  
 233 syngas with 18.5% lower average calorific value than the 30 bar experiment which is primarily related  
 234 to the higher CH<sub>4</sub> content produced at elevated pressures compared to H<sub>2</sub> and CO.

235 Table 4. Average gas compositions obtained in the particular stages of the underground coal  
 236 gasification experiments.

Stage	Gasification reagent	Gas production (Nm <sup>3</sup> /h)	Average gas composition (%)							Average calorific value (MJ/Nm <sup>3</sup> )
			CO <sub>2</sub>	N <sub>2</sub>	H <sub>2</sub>	CH <sub>4</sub>	CO	C <sub>2</sub> H <sub>6</sub>	H <sub>2</sub> S	
<b><i>Atmospheric pressure experiment</i></b>										
I	O <sub>2</sub>	9.16	22.43	0.79	18.73	1.27	56.08	0.13	0.57	9.78
			±1.12	±0.08	±0.94	±0.06	±2.80	±0.01	±0.06	
II	O <sub>2</sub> + H <sub>2</sub> O	9.43	37.01	0.60	25.27	3.40	33.36	0.18	0.18	8.32
			±1.85	±0.03	±1.26	±0.17	±1.67	±0.02	±0.02	
III	Air 6 m <sup>3</sup> /h	8.01	13.47	62.47	13.59	3.34	6.83	0.17	0.13	3.67
			±0.67	±3.12	±0.68	±0.17	±0.34	±0.02	±0.01	
IV	Air 10 m <sup>3</sup> /h	11.87	14.45	70.61	7.66	1.91	5.16	0.14	0.07	2.27
			±0.72	±3.53	±0.38	±0.10	±0.26	±0.01	±0.01	
V	OEA 50%	10.67	31.82	43.66	10.50	1.97	11.90	0.07	0.08	3.41
			±1.59	±2.18	±0.53	±0.10	±0.60	±0.01	±0.01	
VI	OEA 50% + H <sub>2</sub> O	8.79	32.93	43.79	8.48	0.66	14.06	0.03	0.05	2.96
			±1.65	±2.19	±0.42	±0.03	±0.70	±0.01	±0.01	
<b>Total:</b>		<b>9.63</b>	<b>28.85</b>	<b>18.75</b>	<b>18.08</b>	<b>2.30</b>	<b>31.63</b>	<b>0.13</b>	<b>0.26</b>	<b>6.92</b>
			±1.44	±0.94	±0.90	±0.12	±1.58	±0.01	±0.03	
<b><i>High pressure (30 bar) experiment</i></b>										
I	O <sub>2</sub>	8.58	43.77	0.65	14.23	9.62	27.50	0.14	<0.05	8.60
			±2.19	±0.06	±0.71	±0.69	±1.38	±0.01		
II	O <sub>2</sub> + H <sub>2</sub> O	8.64	45.11	0.25	14.64	18.26	20.35	0.95	0.44	11.41
			±2.26	±0.02	±0.73	±0.91	±1.02	±0.10	±0.04	
III	Air 6 m <sup>3</sup> /h	11.24	14.50	58.14	6.03	8.82	10.86	0.93	0.72	5.95
			±0.73	±2.91	±0.30	±0.44	±0.54	±0.09	±0.07	
IV	Air 10 m <sup>3</sup> /h	13.90	13.54	66.78	4.55	5.58	9.13	0.27	0.15	3.85
			±0.68	±3.34	±0.23	±0.28	±0.46	±0.03	±0.02	
V	OEA 50%	14.53	29.58	38.92	8.45	6.68	15.73	0.49	0.15	5.65
			±1.48	±1.95	±0.42	±0.33	±0.79	±0.05	±0.02	
VI	OEA 50% + H <sub>2</sub> O	14.83	29.61	36.98	8.77	6.22	17.40	0.75	0.27	5.92
			±1.48	±1.85	±0.44	±0.31	±0.87	±0.08	±0.03	
<b>Total:</b>		<b>10.48</b>	<b>38.43</b>	<b>16.86</b>	<b>11.97</b>	<b>11.77</b>	<b>20.14</b>	<b>0.58</b>	<b>0.25</b>	<b>8.49</b>
			±1.92	±0.84	±0.60	±0.59	±1.01	±0.06	±0.03	

237 Fig. 7 presents the experimental data provided in the literature on the gas calorific values obtained  
 238 during gasification of coals of different rank using air, OEA and oxygen [19, 21, 23, 26, 27] and the  
 239 comparison with the gas calorific values calculated as a part of this study. Comparing each result  
 240 provided in regard to air gasification, the gas calorific value generally increases with the total carbon  
 241 content in coal, but no precise interdependency can be established as gasification at high pressures  
 242 involved higher air flow rates. The gas calorific values obtained during OEA gasification do not show a  
 243 clear relationship with the total carbon content of coal. This is mainly due to the fact that in each  
 244 experiment reported in the literature, different ratios of oxygen to air were used. Nevertheless, it can

245 be observed in Fig. 7 that the gas calorific values obtained during the OEA gasification as reported in  
 246 the literature and in this work are generally higher than the values obtained during the air gasification.  
 247 In case of oxygen gasification, the values presented in Fig. 7 show that there is a clear increase in the  
 248 gas calorific values with an increase in coal rank. In particular, gasification of semi-anthracite at  
 249 atmospheric conditions as shown in this work can produce a syngas with 2.8 times higher calorific  
 250 value than gasification of lignite coal [19]. In comparison to the bituminous coal [26], an increase of  
 251 21% in calorific value is observed.

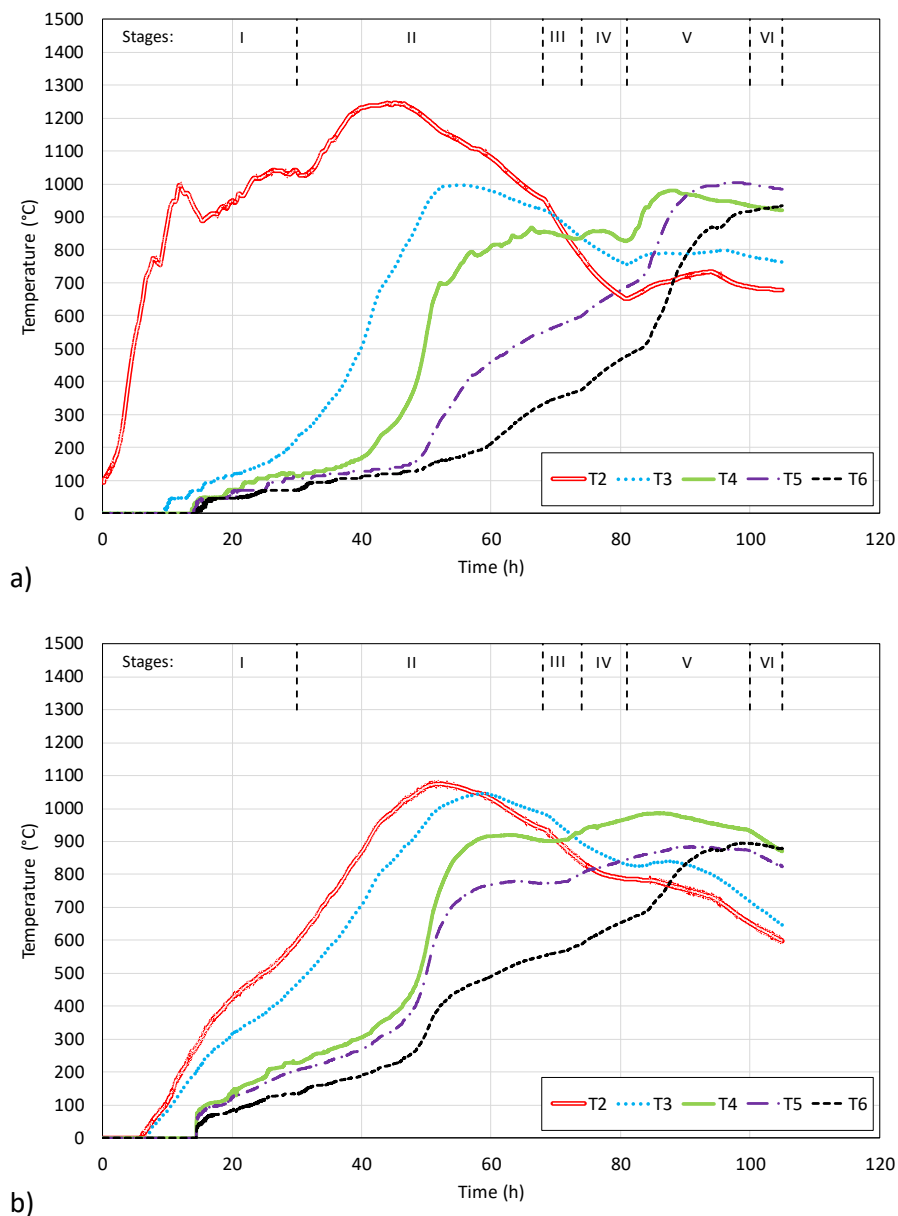


252  
 253 **Fig. 7.** Gas calorific values obtained during gasification of coals of different rank using air, OEA and  
 254 oxygen as reported in the literature and comparison with the results obtained in this work. Values  
 255 above the bars specify flow rates of oxygen and air, and oxygen to air ratios used in the OEA  
 256 experiments.

### 257 3.3. Temperature distribution

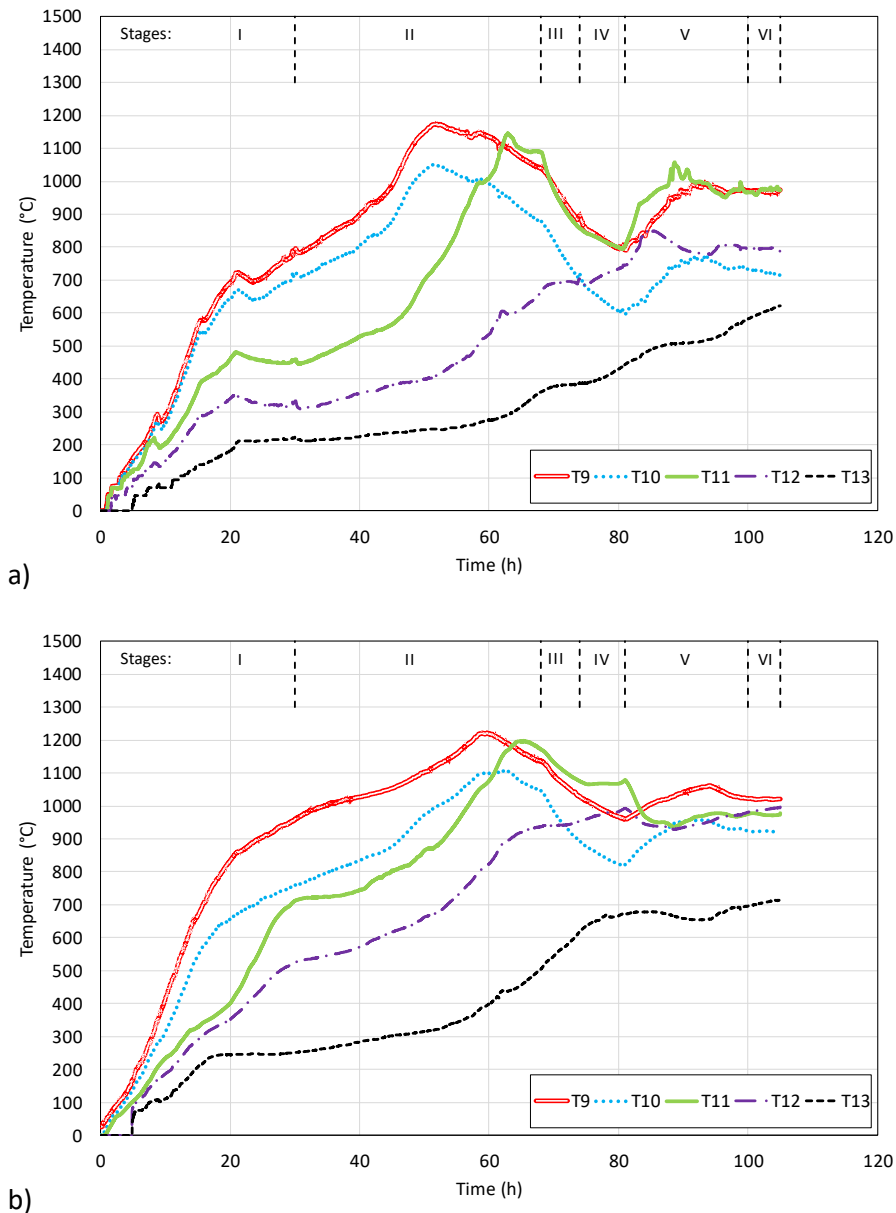
258 The variations of temperature inside the reactor next to the gasification channel for the atmospheric  
 259 and high-pressure experiments are given in Fig. 8a and 8b, respectively. While the temperatures  
 260 recorded by T3-T6 are similar for both experiments, different temperatures between the experiments  
 261 were experienced by thermocouple T2 which was in the proximity of the injection point. In particular,  
 262 the highest temperatures recorded were 1246°C and 1076°C in the atmospheric and high-pressure  
 263 experiments, respectively. Such variation may be attributed to the difference in total rates of oxidation  
 264 reactions, both complete and partial, with carbon. In general, coal combustion reaction phenomena

265 is affected by a number of factors such as coal porosity and its distribution, coal particle size, types  
 266 and contents of specific mineral matter as well as heat and mass transfer conditions in the reactor  
 267 [31]. Such reactions are highly exothermic and consequently, the ratio of the primary products, CO to  
 268 CO<sub>2</sub>, sharply increases with increasing temperature [31]. Values presented in Table 4 confirm this  
 269 phenomenon as the ratio of CO to CO<sub>2</sub> was 2.5 for the atmospheric gasification compared to the ratio  
 270 of 0.6 for the 30 bar experiment.



271 **Fig. 8.** Temperature distributions in the gasification channel over the course of the UCG experiments:  
 272 a) atmospheric gasification, b) high-pressure (30 bar) gasification.

273 The temperature evolutions in the roof of the strata are given in Fig. 9a for the atmospheric pressure  
 274 experiment and in Fig. 9b for the high-pressure experiment. Similar to the temperature measurements  
 275 in the gasification channel, the maximum temperatures in the roof strata were recorded 0.5 m from  
 276 the injection face of the coal seam. However, the temperature of 1222°C recorded in the high-pressure  
 277 experiment was slightly higher than the 1174°C recorded in the atmospheric pressure experiment.



278 **Fig. 9.** Temperature distributions in the roof strata over the course of the UCG experiments: a)  
 279 atmospheric gasification, b) high-pressure (30 bar) gasification.

280 On average in both experiments, the highest temperatures at 0.5 m, 1.0 m and 1.5 m from the  
 281 injection face of the coal seam were recorded during the 2<sup>nd</sup> stage (oxygen and water gasification)

282 followed by a decrease during the air gasification and a slight recovery during the gasification with  
 283 OEA and OEA with water. Temperatures at 2.0 m and 2.5 m from the gas inlet in the roof strata showed  
 284 a continuous increase over the experiment reaching a maximum during the OEA gasification.

285       3.4.       Process balance data

286 Based on the experimental data presented earlier, Table 5 shows calculated values of average  
 287 gasification rates, energy efficiency and average reactor power for particular stages.

288 The 1<sup>st</sup> stage of the atmospheric pressure experiment showed a higher efficiency of 58.35% than the  
 289 2<sup>nd</sup> stage exhibiting 54.25%, which was the opposite for the high-pressure experiment which showed  
 290 an efficiency of 48.56% in the 1<sup>st</sup> stage and 64.08% in the second stage. During air gasification (the 3<sup>rd</sup>  
 291 and 4<sup>th</sup> stages), there was surprisingly an increase in the process energy efficiency up to 73.20% in the  
 292 atmospheric pressure test and 79.36% in the high-pressure test, despite the decrease in the gas  
 293 calorific values. This can be attributed to the relatively short duration of the air gasification stages (13  
 294 hours in total) as well as the accumulated thermal energy from the 2<sup>nd</sup> stage. Similar to the first two  
 295 stages, the gasification with OEA under atmospheric pressure conditions showed higher efficiency  
 296 (35.83%) than the gasification with OEA and water (30.29%). The opposite was observed in the high-  
 297 pressure experiment, where the OEA and water yielded a higher energy efficiency (52.10%) than the  
 298 OEA gasification (51.21%). In total, energy efficiency of the gasification at 30 bar is 57.67% which is  
 299 higher compared to the atmospheric pressure gasification efficiency of 51.72%.

300 Table 5. Mass and energy balance calculations for particular stages of the underground coal  
 301 gasification experiments.

Stage	Gasification reagent	Total gas yield (Nm <sup>3</sup> )	Energy in process gas (MJ)	Average reactor power (kW)	Gasification rate (kg/h)	Energy in coal consumed (MJ)	Energy efficiency (%)
<b><i>Atmospheric pressure experiment</i></b>							
I	Oxygen	274.64	2670.70	24.73	4.51	4576.84	58.35
II	Oxygen + water	358.24	2999.80	21.96	4.30	5529.81	54.25
III	Air 6 m <sup>3</sup> /h	48.06	175.67	8.14	1.18	239.98	73.20
IV	Air 10 m <sup>3</sup> /h	83.06	190.32	7.48	1.59	377.04	50.48
V	OEA 50%	202.77	693.31	10.15	3.01	1935.07	35.83

VI	OEA 50% + water	43.94	132.22	7.30	2.58	436.53	30.29
Total:		1010.68	6862.02	18.15	3.37	1326.97	51.72
<b>High-pressure (30 bar) experiment</b>							
I	Oxygen	257.51	2219.08	20.48	4.50	4569.79	48.56
II	Oxygen + water	328.22	3750.84	27.42	4.55	5853.49	64.08
III	Air 8 m <sup>3</sup> /h	67.45	401.64	18.59	2.49	506.11	79.36
IV	Air 12 m <sup>3</sup> /h	97.32	378.07	15.02	2.46	583.31	64.80
V	OEA 50%	276.14	1559.49	22.80	4.74	3045.03	51.21
VI	OEA 50% + water	74.15	440.26	24.46	5.02	845.04	52.10
Total:		1100.79	8449.31	23.15	4.34	15402.76	57.67

## 302 4. Conclusions

303 The experiments conducted demonstrated a significant influence of the gasifying medium used and  
304 applied pressure regime (atmospheric pressure and 30 bar pressure gasification) on the UCG gas  
305 composition and overall process efficiency. Hence, the following conclusions can be made:

- 306 • Although the gas from the gasification process at 30 bar using O<sub>2</sub> as a reactant contained more  
307 CH<sub>4</sub> compared to the atmospheric pressure gasification, as the methanation and  
308 hydrogasification reactions are favoured at high pressures, it contained less H<sub>2</sub> and CO leading  
309 to slightly lower calorific value in the 30 bar experiment. This was mainly attributed to the  
310 higher temperature near the reactor inlet during atmospheric gasification, caused by  
311 variations in total rates of oxidation reactions and benefiting Boudouard, gas-shift and steam  
312 gasification reactions to enhance the production of H<sub>2</sub>, CO and CO<sub>2</sub>.
- 313 • Injection of water in the 2<sup>nd</sup> stage led to a decrease in CO content and an increase in the  
314 content of CO<sub>2</sub>, H<sub>2</sub> and CH<sub>4</sub> in both experiments, however, the observed changes were more  
315 pronounced for the high-pressure process.
- 316 • During the air gasification stages, an increase in the process energy efficiency was observed  
317 compared to previous stages with oxygen and water, although the gas caloric value decreased  
318 in both experiments. Injection of OEA and adding water to it subsequently resulted in  
319 improvement of gas quality but reduced the gasification efficiency in both experiments.  
320 However, if the results are calculated on a N<sub>2</sub>-free basis, one could infer that the gas calorific

321 value of air gasification stages are similar, or even higher for the 30 bar gasification, to both  
322 the stages where oxygen and OEA were injected. Such behaviour can be attributed to the  
323 relatively short duration of the air gasification stages and the fact that the reactor had an  
324 accumulated thermal energy from the stages where oxygen was the main reactant.

325 • The overall energy efficiency of the high pressure (30 bar) experiment was higher compared  
326 to the atmospheric pressure test, i.e. 57.67% compared to 51.72%. This was mainly due to  
327 higher methane concentrations in gas obtained during the high-pressure experiment.

328 • Under elevated pressure, the temperatures recorded in the roof strata were higher compared  
329 to the atmospheric gasification, while the opposite was observed in the gasification channel.

330 The differences may have resulted from different total rates of oxidation reactions and  
331 variations in fluid flow patterns in the gasification chamber during the two experiments, which  
332 influenced the heat transport due to convection. Additionally, heat insulating effects of coal  
333 ash remaining in the gasification channel could take place. The distribution of ash strongly  
334 depends on the fluid flow conditions in the reaction chamber and on the distribution of ash in  
335 the raw coal sample.

336 • By comparing the results of this work with the available literature data, it can be concluded  
337 that there is an increase in the gas calorific values with an increase in coal rank, as syngas with  
338 more than 280% and 20% higher calorific value can be obtained by gasification of semi-  
339 anthracite compared to lignite and bituminous coals, respectively.

340 • The conditions simulated in the reactor are similar to those during the Linked Vertical Wells  
341 (LVW) process. As a consequence, a gradual deterioration of the gas quality is observed during  
342 the experiments. This resulted in the elaboration of CRIP technique, in which a new reactor is  
343 started when the gas quality decreases. The obtained results suggest that the proper  
344 manipulation in reactant dosing may practically help in more stable gas quality in CRIP as well  
345 as in LVW technique. In those techniques the gas calorific value decreases as the cavity is  
346 growing so to counteract such phenomenon, the changes in the gasification reagent could be

347 helpful. It is extremely important not to exceed the hydrostatic pressure of the surrounding  
348 to avoid pressure losses and gas leakages.

- 349 • The main factors influencing the gas composition are the gasification reagent used and long-  
350 term stability of the gasification conditions. In order to obtain stable syngas quality in terms  
351 of its calorific value, it is important to provide an appropriate amount of oxidant to the reactor.  
352 The best reagent to obtain a high calorific gas during UCG is the mixture of oxygen and water  
353 unless natural water is available in excess quantities. A gradual decrease in the gas calorific  
354 value, however, cannot be avoided during operation of a single reactor, so retracting the  
355 oxygen injection point (CRIP technique) would be necessary to maintain the process at the  
356 desired parameters.

## 357 5. Acknowledgements

358 This work was carried out as a part of the FLEXIS project which has been part-funded by the European  
359 Regional Development Fund through the Welsh Government. The financial support, for the first two  
360 authors, is gratefully acknowledged.

## 361 6. References

- 362 1. IPCC. The Intergovernmental Panel on Climate Change, *Global warming of 1.5°C. An IPCC*  
363 *Special Report*. 2018.
- 364 2. The Royal Society and Royal Academy of Engineering, *Greenhouse gas removal*. Report, 2018.
- 365 3. International Energy Agency (IEA), *World Energy Outlook 2018*. 2018.
- 366 4. International Energy Agency (IEA). *Carbon Capture and Storage: The solution for deep*  
367 *emissions reductions*. 2015. IEA.
- 368 5. Shafirovich, E. and A. Varma, *Underground coal gasification: a brief review of current status*.  
369 *Industrial & Engineering Chemistry Research*, 2009. **48**(17): p. 7865-7875.
- 370 6. Thomas, H., et al. *Deep Ground and Energy: Carbon Sequestration and Coal Gasification*. in  
371 *The International Congress on Environmental Geotechnics*. 2018. Springer.
- 372 7. Bhutto, A.W., A.A. Bazmi, and G. Zahedi, *Underground coal gasification: From fundamentals*  
373 *to applications*. *Progress in Energy and Combustion Science*, 2013. **39**(1): p. 189-214.
- 374 8. Perkins, G., *Underground coal gasification—Part I: Field demonstrations and process*  
375 *performance*. *Progress in Energy and Combustion Science*, 2018. **67**: p. 158-187.
- 376 9. Wang, F., *Comparison of analytical methods for phenols, cyanide, and sulfate as applied to*  
377 *groundwater samples from underground coal gasification sites*, in *Analysis of Waters*  
378 *Associated with Alternative Fuel Production*. 1980, ASTM International.
- 379 10. Thorsness, C. and J. Britten, *Lawrence Livermore National Laboratory Underground Coal*  
380 *Gasification project*. 1989, Lawrence Livermore National Lab., CA (USA).

- 381 11. Dennis, D., *Rocky Mountain 1 underground coal gasification test project Hanna*. 2006,  
382 Wyoming, Final technical report for the Period 1986 to 2006. National Energy Technology  
383 Laboratory.
- 384 12. Chandelle, V., et al. *Overview about Thulin Field Test*. in *Proceedings of the Twelfth Annual*  
385 *Underground Coal Gasification Symposium, Saarbrucken, Germany*. 1986.
- 386 13. Chappell, B. and M. Mostade. *The El Tremedal underground coal gasification field test in*  
387 *Spain—First trial at great depth and high pressure*. in *Fifteenth annual international Pittsburgh*  
388 *coal conference*. 1998.
- 389 14. Wiatowski, M., et al., *Technological aspects of underground coal gasification in the*  
390 *Experimental “Barbara” Mine*. *Fuel*, 2015. **159**: p. 454-462.
- 391 15. Mao, F., *Underground coal gasification (UCG): a new trend of supply-side economics of fossil*  
392 *fuels*. *Natural Gas Industry B*, 2016. **3**(4): p. 312-322.
- 393 16. Blinderman, M. and R. Jones. *The Chinchilla IGCC project to date: Underground coal*  
394 *gasification and environment*. in *Proceedings of the Gasification Technologies Conference, San*  
395 *Francisco, CA, USA*. 2002.
- 396 17. Olness, D., *The Angrenskaya underground coal gasification station*. Vol. 53300. 1982:  
397 Lawrence Livermore Laboratory.
- 398 18. Stańczyk, K., et al., *Dynamic experimental simulation of hydrogen oriented underground*  
399 *gasification of lignite*. *Fuel*, 2010. **89**(11): p. 3307-3314.
- 400 19. Stańczyk, K., et al., *Gasification of lignite and hard coal with air and oxygen enriched air in a*  
401 *pilot scale ex situ reactor for underground gasification*. *Fuel*, 2011. **90**(5): p. 1953-1962.
- 402 20. Stańczyk, K., et al., *Experimental simulation of hard coal underground gasification for*  
403 *hydrogen production*. *Fuel*, 2012. **91**(1): p. 40-50.
- 404 21. Kapusta, K., M. Wiatowski, and K. Stańczyk, *An experimental ex-situ study of the suitability of*  
405 *a high moisture ortho-lignite for underground coal gasification (UCG) process*. *Fuel*, 2016. **179**:  
406 p. 150-155.
- 407 22. Laciak, M., et al., *The analysis of the underground coal gasification in experimental equipment*.  
408 *Energy*, 2016. **114**: p. 332-343.
- 409 23. Gur, M., et al., *Experimental results of underground coal gasification of Turkish lignite in an*  
410 *ex-situ reactor*. *Fuel*, 2017. **203**: p. 997-1006.
- 411 24. Wang, Z., et al., *Expansion of three reaction zones during underground coal gasification with*  
412 *free and percolation channels*. *Fuel*, 2017. **190**: p. 435-443.
- 413 25. Su, F.-q., et al., *Evaluation of a Compact Coaxial Underground Coal Gasification System Inside*  
414 *an Artificial Coal Seam*. *Energies*, 2018. **11**(4): p. 898.
- 415 26. Wiatowski, M., et al., *Ex-situ experimental simulation of hard coal underground gasification at*  
416 *elevated pressure*. *Fuel*, 2016. **184**: p. 401-408.
- 417 27. Wiatowski, M., et al., *Efficiency assessment of underground gasification of ortho-and meta-*  
418 *lignite: High-pressure ex situ experimental simulations*. *Fuel*, 2019. **236**: p. 221-227.
- 419 28. Konstantinou, E. and R. Marsh, *Experimental study on the impact of reactant gas pressure in*  
420 *the conversion of coal char to combustible gas products in the context of Underground Coal*  
421 *Gasification*. *Fuel*, 2015. **159**: p. 508-518.
- 422 29. Sadasivam, S., et al., *Experimental study of methane-oriented gasification of semi-anthracite*  
423 *and bituminous coals using oxygen and steam in the context of underground coal gasification*  
424 *(UCG): Effects of pressure, temperature, gasification reactant supply rates and coal rank*. *Fuel*,  
425 2020. **268**: p. 117330.
- 426 30. ASTM Standards, *ASTM D388. Standard Classification of Coals by Rank*. ASTM International,  
427 2015. **05.06**(West Conshohocken, PA).
- 428 31. Lee, S., J.G. Speight, and S.K. Loyalka, *Handbook of alternative fuel technologies*. 2014: crc  
429 Press.